



Concurrent recovery of ammonia and phosphate by an electrochemical nutrients recovery system with authigenic acid and base

Zuobin Wang^{a,b}, Zhiqiang Zhang^{a,b,*}, Jiao Zhang^{c,*}, Lu She^{a,b,d}, Pengyu Xiang^e, Siqing Xia^{a,b}

^a State Key Laboratory of Pollution Control and Resource Reuse, Key Laboratory of Yangtze River Water Environment, Ministry of Education, College of Environmental Science and Engineering, Tongji University, Shanghai 200092, China

^b Shanghai Institute of Pollution Control and Ecological Security, Shanghai 200092, China

^c School of Municipal and Ecological Engineering, Shanghai Urban Construction Vocational College, Shanghai 200432, China

^d Central-Southern Safety & Environment Technology Institute Co., Ltd., Wuhan 430061, China

^e Zhejiang Weiming Environment Protection Co., Ltd., Wenzhou 325000, China

ARTICLE INFO

Keywords:

Ammonia recovery
Phosphate recovery
Electrochemical system
Transmembrane chemisorption
Hydroxyapatite crystallization

ABSTRACT

Strong wastewater containing ammonia and phosphate is anticipated to become potential sources of nutrient elements (N and P). However, high N/P molar ratios in most kinds of strong wastewater make it difficult to realize simultaneous and full recovery of N and P. Thereout, the present study developed an electrochemical nutrients recovery system (ECNRS) with authigenic acid and base to integrate transmembrane chemisorption and hydroxyapatite crystallization for concurrent N and P recoveries from wastewater. Compared with separate N or P recovery, the concurrent recovery of N and P in the ECNRS could obviously enhance N and P recovery efficiencies. Under 4.0 V applied voltage and 12 h operation, the ECNRS recovered 79.2% of N and 100% of P, which were higher than those of separated N or P recovery. However, increasing influent N or P concentration would prolong recovery time for the nutrients, which might be attributed to the enhanced pH buffering of catholyte with high influent concentration. Energy consumption for N recovery was 14.6 kWh/kg N with a flux of 47.3 g NH₃-N/(m²·d). Economic costs for N and P recovery via the ECNRS were 1.84 \$/kg N and 0.69 \$/kg P, respectively. Considering the concurrent N and P recovery via ECNRS, the obtained preliminary profit rate could be over 300%. The developed system with concurrent N and P recoveries showed a cost-effective advantage.

1. Introduction

Nitrogen (N) and phosphorus (P) are both essential elements for plants growth and hence are widely used in agriculture as fertilizers. However, N is utilized by the conversion of atmosphere N₂ into ammonia (NH₃-N) by Haber-Bosch process, which is energy intensive with 9.1–14.3 kWh/kg N, average 6.9 kg CO₂-equivalent (CO₂-eq)/kg N synthesis [1]. Moreover, P is majorly extracted from P rock, which is a limited and nonrenewable resource. Both the consumption and the demand of P are increasing year-by-year [2]. The crisis that P rock reserves will be depleted in the near 50–100 years has become one of the most concerned issues among researchers [3–6]. Meanwhile, a substantial part of N and P end up in wastewater. The quantity of ammonium (NH₄⁺-N) in domestic wastewater is equivalent to 19% of the annual NH₃-N

production [7]. Conventionally, NH₄⁺-N is removed from wastewater by nitrification and denitrification (N/DN) with an energy consumption of 16 kWh/kg N. Another challenge is the generation and emission of N₂O, which contribute 80% of the total greenhouse gas emissions of wastewater treatment plants [7,8]. P contained in domestic wastewater accounts for 22% of the world's consumption, and most of them end in the form of phosphate (H₂PO₄⁻, HPO₄²⁻, PO₄³⁻), which can be regarded as a potential P source reservoir [9]. Thus, nutrients recovery from wastewater has inevitably become the tendency to pursue sustainable N and P utilization.

Many kinds of strong wastewater, such as source-separated urine, sludge digestate and animal manure digestate, contain ample N and P, which are anticipated to become important potential nutrients sources. However, the general objective of most wastewater treatment facilities

* Corresponding authors at: State Key Laboratory of Pollution Control and Resource Reuse, Key Laboratory of Yangtze River Water Environment, Ministry of Education, College of Environmental Science and Engineering, Tongji University, Shanghai 200092, China (Z. Zhang). School of Municipal and Ecological Engineering, Shanghai Urban Construction Vocational College, Shanghai 200432, China (J. Zhang).

E-mail addresses: zhiqiang@tongji.edu.cn (Z. Zhang), zhangjiao@succ.edu.cn (J. Zhang).

<https://doi.org/10.1016/j.cej.2022.140169>

Received 10 August 2022; Received in revised form 29 September 2022; Accepted 30 October 2022

Available online 4 November 2022

1385-8947/© 2022 Elsevier B.V. All rights reserved.

is to remove N and P regarding them as waste via various methods, ignoring their resource attribution. Nutrient bioaccumulation by autotrophic microorganisms such as microalgae is one of the technologies for N and P recoveries [10]. Nevertheless, the microalgae are hard to be harvested due to their poor settling properties, increasing the operation cost for their harvesting and dewatering [11]. Although air stripping or steam stripping could capture N from the wastewater, they need to consume a lot of chemical agents (e.g., acid and base) and energy. Struvite ($\text{MgNH}_4\text{PO}_4 \cdot 6\text{H}_2\text{O}$) crystallization is one of the widely studied chemical precipitation methods for synchronous recovery of N and P from waste streams. The cost of struvite crystallization is mainly dependent on the magnesium and base sources, which could contribute to 75 % of overall costs [12]. Moreover, struvite crystallization is better fit for P recovery than for N recovery, since N molar concentration is usually 10 times over than P molar concentration in most of strong wastewater [13]. Taking urine as an example, there was over 200 mM N and less than 10 mM P in it. Therefore, it is of big significance to develop an alternative method for simultaneous and full recovery of N and P.

Due to the big demands for acid and base in the N and P recoveries process, electrochemical systems (ES) and bioelectrochemical systems (BES) have been proposed as energy efficient alternatives to recover N and P from wastewater [14–17]. In most studies, researchers just utilized the hydroxide ions which were generated at the cathode as the base source of ammonia stripping or phosphate crystallization. In our previous studies, we reported two (bio)electrochemical systems aimed for nutrients recovery from wastewater which were called bioelectrochemical membrane-absorbed ammonia (BEMAA) system and microbial electrolysis phosphorus-recovery cell (MEPRC), respectively [18,19]. The BEMAA could capture N via transmembrane chemisorption (TMCS) with authigenic acid and base, while the MEPRC could recover P via hydroxyapatite (HAP) crystallization. The demands for chemical agents and energy were greatly reduced due to the authigenic acid and base in the (bio)electrochemical systems. Since high N/P molar ratios in most kinds of strong wastewater make it difficult to realize simultaneous and efficient N and P recover, it would be of great significance to explore integrating TMCS and HAP crystallization into one system to achieve concurrent N and P recoveries.

In this study, we developed an electrochemical nutrients recovery system (ECNRS), which integrated the two processes of TMCS and HAP crystallization. Its characteristics of recovering N and P were investigated in detail. The specific investigations involved the following aspects: (i) separate N recovery and separate P recovery in the ECNRS; (ii) concurrent N and P recoveries in the ECNRS; (iii) key factors for the concurrent N and P recoveries; (iv) energy consumption and preliminary economic analyses of the concurrent N and P recoveries in the ECNRS.

2. Materials and methods

2.1. Solution synthesis

The electrolyte was prepared with $(\text{NH}_4)_2\text{SO}_4$ and Na_2SO_4 . N & P-rich solution was prepared with $(\text{NH}_4)_2\text{SO}_4$, $\text{NaH}_2\text{PO}_4 \cdot 2\text{H}_2\text{O}$ and $\text{Ca}(\text{NO}_3)_2 \cdot 4\text{H}_2\text{O}$. All the chemical reagents used in this study are of analytical grade and purchased from Sinopharm Chemical Reagent Co., Ltd.

2.2. ECNRS construction

The ECNRS consisted of five chambers. The scheme of the ECNRS was shown in Fig. S1. The anode chamber (AnC), acid-production chamber (AcC), desalination chamber (DeC) and absorption chamber (AbC) were all in the dimensions of $8\text{ cm} \times 8\text{ cm} \times 1.5\text{ cm}$ while the cathode chamber (CaC) was in the dimension of $8\text{ cm} \times 8\text{ cm} \times 3\text{ cm}$. All the five chambers were made of polycarbonate. Silicone sheets were set between every-two chambers to ensure the sealing, which resulted in 200 cm^3 net volume of cathode chamber and 100 cm^3 net volume of

other chambers. Two pieces of cation exchange membranes (CEM, CMI-7000, Membranes International Inc., New Jersey, USA) were placed between AnC and AcC, DeC and CaC, respectively. An anion exchange membrane (AEM, AMI-7001, Membranes International Inc., New Jersey, USA) was placed between AcC and DeC. A hydrophobic gas permeable membrane (GPM; $0.22\text{ }\mu\text{m}$ pore size, $150\text{--}190\text{ }\mu\text{m}$ thickness, PP-supporting PTFE; Membrane Solutions Inc, China) was set between CaC and AbC. The ECNRS contained an anode and a cathode. The anode was a titanium plate coated with iridium oxide and ruthenium oxide ($3\text{ cm} \times 5\text{ cm}$). The cathode was made of stainless-steel mesh (Type 304, $8\text{ cm} \times 8\text{ cm}$).

2.3. ECNRS operation

The synthetic N & P-rich solution was added into the CaC and was circulated by a peristaltic pump with a rate of $70\text{ mL}/\text{min}$ (BT100-2 J, Longer Precision Pump Co., Ltd., China). $300\text{ mM Na}_2\text{SO}_4$ solution was added into the DeC. The remaining chambers were filled with $6.0\text{ mM} (\text{NH}_4)_2\text{SO}_4$ solution as electrolyte. The voltage of 3.0 V was applied to the ECNRS by using a power supply (Array Electronics Co., Ltd., Nanjing, China). A $10\text{-}\Omega$ resistance was connected in the external circuit to record the voltage used for current calculation. The voltage across the resistance was recorded every 5 min by using a multimeter (Keithley Model 2700, Tektronix, USA). All the experiments were operated in a 24-h duration at $25.0 \pm 1.0\text{ }^\circ\text{C}$ temperature. The detailed information of all experiments was summarized in Table S1.

2.4. Analyses of liquid and solid phases

Liquid samples collected from the cathode chamber were filtered through a $0.22\text{-}\mu\text{m}$ microfiltration membrane and then determined N and P concentration by using a spectrophotometry (UV-2700, Shimadzu, Kyoto, Japan). The catholyte pH was monitored by using a pH probe (E-201-C, Leici, Shanghai, China). The precipitates collected from the cathode chamber was characterized by using scanning electron microscope (SEM; Phenom Prox, Phenom, Eindhoven, Netherlands), Energy dispersive spectroscopy (EDS; Phenom Prox, Phenom, Eindhoven, Netherlands) and X-ray diffraction (XRD; D8 Advance, Bruker Corporation, Karlsruhe, Germany).

2.5. Calculations

Nitrogen recovery efficiency (E_N , %) is calculated as Eq. (1):

$$E_N = \frac{c_N^0 - c_N^e}{c_N^0} \times 100\% \quad (1)$$

where c_N^0 (mg/L) and c_N^e (mg/L) are the initial and the end nitrogen concentration in the cathode chamber, respectively.

Phosphorus recovery efficiency (E_P , %) is calculated as Eq. (2):

$$E_P = \frac{c_P^0 - c_P^e}{c_P^0} \times 100\% \quad (2)$$

where c_P^0 (mg/L) and c_P^e (mg/L) are the initial and the end phosphate concentration in the cathode chamber, respectively.

The energy consumption (EC , kWh/kg N or kWh/kg P) of N and P recoveries are calculated as our previous report [18]. Carbon emission (CE , kg $\text{CO}_2\text{-eq}/\text{kg N}$) for N recovery was expressed by GHG emission and calculated by the following:

$$CE = k \times EC \quad (3)$$

where k (kg $\text{CO}_2\text{-eq}/\text{kWh}$) is the GHG emission factor for electricity and it is set as 0.65 in this study [20].

And the total economic cost of the concurrent N and P recoveries was calculated as the following:

$$C_t = C_c + C_e \quad (4)$$

where C_t (\$/kg N or \$/kg P) is the total cost of the concurrent N and P recoveries, C_c (\$/kg N or \$/kg P) is the cost of the chemical reagents, C_e (\$/kg N or \$/kg P) are the electric cost of the reactor and the pumps respectively.

The economic benefit (E_{profit} , %) of concurrent N and P recovery via was preliminarily calculated by Eq. (5):

$$E_{profit} = \frac{\sum_j R_j p_j - (c_{electricity} \times P_{electricity} + \sum_k c_k p_k)}{c_{electricity} \times P_{electricity} + \sum_k c_k p_k} \times 100\% \quad (5)$$

where R_j (kg) is the recovery amount of N or P and p_j (\$/kg) are the prices of recovery product in the forms of $(\text{NH}_4)_2\text{SO}_4$ and HAP; $c_{electricity}$ (kWh) and $P_{electricity}$ are the consumption amount and price of the electricity power; c_k (kg) and p_k (\$/kg) are the consumption amount and prices of the chemical agent in the forms of $(\text{NH}_4)_2\text{SO}_4$ and $\text{Ca}(\text{OH})_2$.

3. Results and discussion

3.1. Separate N or P recovery in the ECNRS

We first investigated the separate N or P recovery performance of the ECNRS at 4.0 V applied voltage. In the separate N recovery experiments, Fig. 1a shows that the catholyte pH in the CaC rose to 12 within 4 h, which was higher than pH 9.3 required for the ammonium-ammonia transformation. The electrolyte pH in the AbC (or AcC) decreased during the operation and was below 4. The pH conditions in the CaC and AbC could stratify the ammonium-ammonia transformation and the transmembrane chemisorption at the same time. Based on this, over 80% of ammonia was absorbed and recovered in the AbC and AcC (Fig. 1b). The ammonia recovery in the ECNRS could include three steps: (i) in the catholyte, pH was raised by the Faradic reaction on the cathode surface, and NH_4^+ was transformed into $\text{NH}_3(\text{g})$ then diffused to the CaC side interface of the GPM; (ii) $\text{NH}_3(\text{g})$ transferred across the GPM to the AbC side of the GPM driven by partial pressure difference of $\text{NH}_3(\text{g})$ over the membrane; (iii) the $\text{NH}_3(\text{g})$ reacted with H^+ on the AbC side of the GPM and was chemically trapped as NH_4^+ . On the other hand, the N removal efficiency in the CaC was over 95%. According to the N distribution (Fig. S2), a little portion of N transferred into the DeC via back diffusion due to the concentration gradient, which resulted in the difference between the recovery and removal efficiencies [19].

In the separate P recovery experiments, the applied voltage was set at 3.0 V. The catholyte pH was elevated to about 14 and over 80% of P was recovered within 4 h (Fig. 2). The P recovery efficiency firstly rose, then slightly decreased, and finally stabilized at about 80% with 24 h operation (Fig. 2b). The XRD, SEM and EDS spectra testified that the 24 h

recovery product mainly consisted of HAP (Fig. S3). There might be a transformation procedure from amorphous calcium phosphate (ACP) to HAP, and this procedure could release a little PO_4^{3-} which led to the slight drop of the recovery efficiency [18].

3.2. Concurrent N and P recoveries in the ECNRS

3.2.1. Performance of the system

In consideration of that the recoveries of N and P mainly occurred within the former 12 h, the results of 12 h operation were discussed in the following sections. Synthetic N & P rich solution was added into the CaC to investigate the concurrent N and P recoveries performance of the ECNRS at 4.0 V applied voltage. The catholyte pH rose to 11 in 12 h (Fig. S4a), but the rising speed was slower than that in the separate N or P recovery experiments. The current density was over 16 A/m^2 , and its consistence in the two cycles indicated the stability of the system (Fig. S4b). The N recovery efficiency was $79.2 \pm 3.5\%$, which were higher than that ($63.7 \pm 3.2\%$ within 12 h) in the separate N recovery experiments (Fig. 3a). The P recovery was enhanced in the concurrent N and P recoveries process. The P recovery efficiency reached to about 95% within 4 h, and all of the P in the catholyte was nearly recovered after 8 h (Fig. 3b). From Fig. S4a, both the CaC pH rising and the AcC & AbC pH decreasing were slowed down, and the final pHs were not as extreme high or low and those in the separate recovery processes (Fig. 1a and Fig. 2a). It indicates that the utilizations of both OH^- ions and H^+ ions were obviously enhanced, and more of them took part in the recovery chemical reactions. Accordingly, the concurrent N and P recoveries in the ECNRS showed higher recovery efficiencies than the separate N or P recovery processes.

3.2.2. Effects of influent N concentration on the concurrent N and P recoveries

The effects of influent N concentration (40 mM, 80 mM and 200 mM ammonium) on the concurrent N and P recoveries were investigated. A significant decrease (from $94.1 \pm 1.4\%$ to $57.9 \pm 2.0\%$) of N recovery efficiency was observed when the influent N concentration increased (Fig. 4a). On the other hand, the absolute recovery quantity of N increased from $122.6 \pm 1.3 \text{ mg}$ to $268.9 \pm 6.6 \text{ mg}$ (Fig. 4b), which was consistent with our previous study [19].

The change of the influent N concentration has a significant effect on the catholyte pH (Fig. 4c). High influent N concentration resulted in slow pH elevation due to the buffering capacity of NH_4^+ ions. When the influent N concentration was 200 mM, the bulk pH in the CaC was below 9 which was lower than the dissociation constant of NH_4^+ ($\text{p}K_a(\text{NH}_4^+) = 9.3$). This indicated that local higher pH near the cathode might drive the conversion from NH_4^+ to free ammonia.

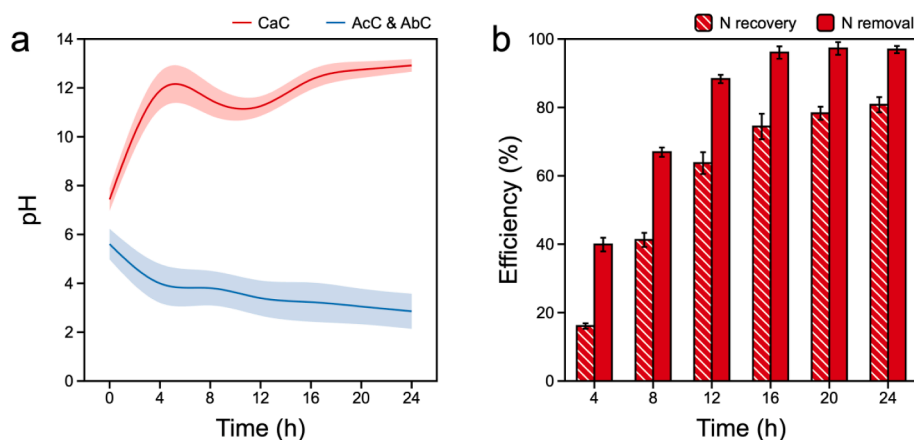


Fig. 1. (a) Electrolyte pHs in the CaC, AcC and AbC; (b) N recovery and removal efficiencies of the ECNRS for the separate N recovery experiments. (80 mM N and 4.0 V applied voltage).

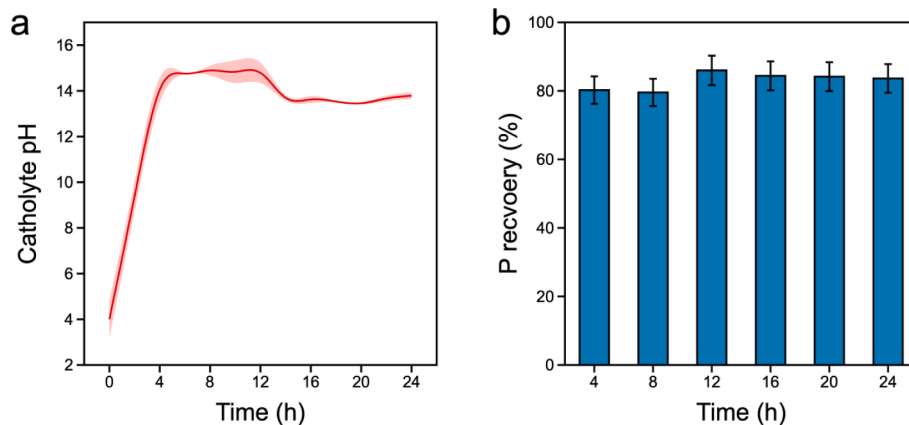


Fig. 2. (a) Electrolyte pH in the CaC and (b) P recovery efficiencies of the ECNRS for the separate P recovery experiments within 24 h. (5 mM P, Ca/P = 2:1, and 3.0 V applied voltage).

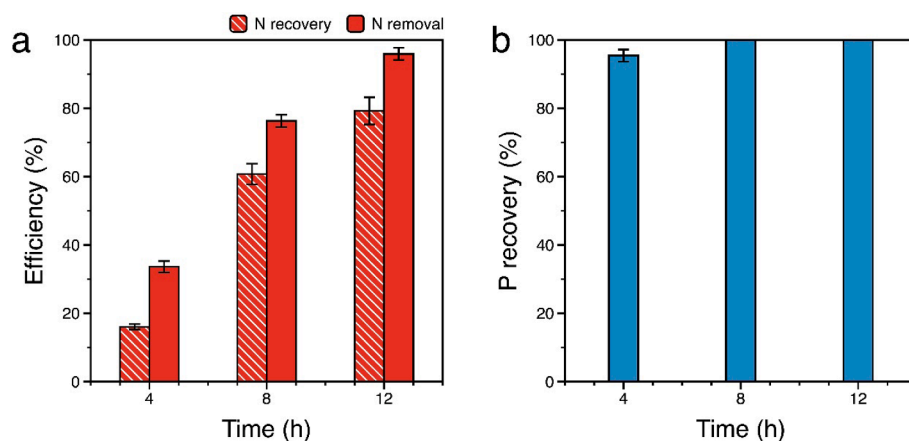
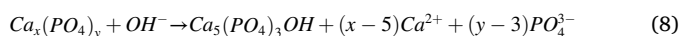


Fig. 3. (a) N recovery and removal efficiencies; and (b) P recovery efficiencies of the ECNRS for the concurrent N and P recovery experiments within 12 h. (80 mM N, influent 5 mM P, Ca/P = 2:1, and 4.0 V applied voltage).

Thus, we calculated the local pH near the cathode according to Eq. (6) - Eq. (7). As the subgraph of Fig. 4c showed, the local pH of the cathode surface could range from 10.4 to 11.4 based on the thickness of the diffusion layer over the cathode, which satisfied the conditions of the ammonium-ammonia transformation. The influent N concentration seemed to have insignificant effect on the P recovery efficiency (Fig. 4d). However, the decreased bulk pH might affect CaP precipitation behavior. Even though the local pH might drive precipitation generation in the electrochemical induced CaP crystallization process, the lack of OH⁻ in the bulk could hinder the further CaP precipitation (e.g., transforming to HAP in Eq. (8)) [21].

$$i_c = \frac{nFD\Delta C_{OH^-}}{1000\delta} \quad (6)$$

$$pH = 14 - p(10^{pH_{bulk}-14} + \Delta C_{OH^-}) \quad (7)$$



where i_c (A/cm²) is the current density, and the average current density (1.64×10^{-3} A/cm²) is assigned to i_c ; n is the number of transferred electrons per unit of OH⁻ generated; D is the diffusion constant of OH⁻ (6.65×10^{-5} cm²/s); ΔC_{OH^-} (mol/L) is the change of OH⁻ concentration across the diffusion layer near the cathode; and δ (cm) is the diffusion layer thickness which has been estimated to 10 ~ 100 μ m [22].

3.2.3. Effects of influent P concentration on the concurrent N and P recoveries

The effect of influent P concentration (2 mM, 5 mM and 10 mM phosphate) was discussed in this section. Increasing the influent P concentration seemed to have little influence on the P recovery efficiency, but higher influent P concentration resulted in the increased P recovery quantity (from 12.2 ± 0.7 mg to 52.8 ± 2.9 mg) (Fig. 5a-b). When the influent P concentration was 2 mM, the P recovery efficiency was lower than that of high influent P concentration in the early 8 h. According to the saturation index of HAP in the variable P concentration (Fig. 5c), higher pH was required to be oversaturation when the P concentration was 2 mM, which could explain the lower efficiency in the early 8 h. The N recovery efficiency decreased from $84.4 \pm 4.2\%$ to $68.4 \pm 2.2\%$ when the initial influent P concentration increased from 2 mM to 10 mM (Fig. 5d).

The electrolyte pH in the AbC barely changed when we changed the influent P concentration (Fig. S5), and thus the stable absorbent pH had less effect on the N recovery performance in the ammonia membrane stripping process [23]. As the previous report, high P concentration could delay the pH elevation, this might lead to the N recovery efficiency decreasing [18]. NH₄⁺ ions in the catholyte could gather at the cathode-solution interface via diffusion and migration and be converted into free NH₃ under the local high pH condition [24]. The NH₃ need to migrate across the electrode-membrane space to membrane interface before the transmembrane chemisorption process. In this migration, NH₃ was

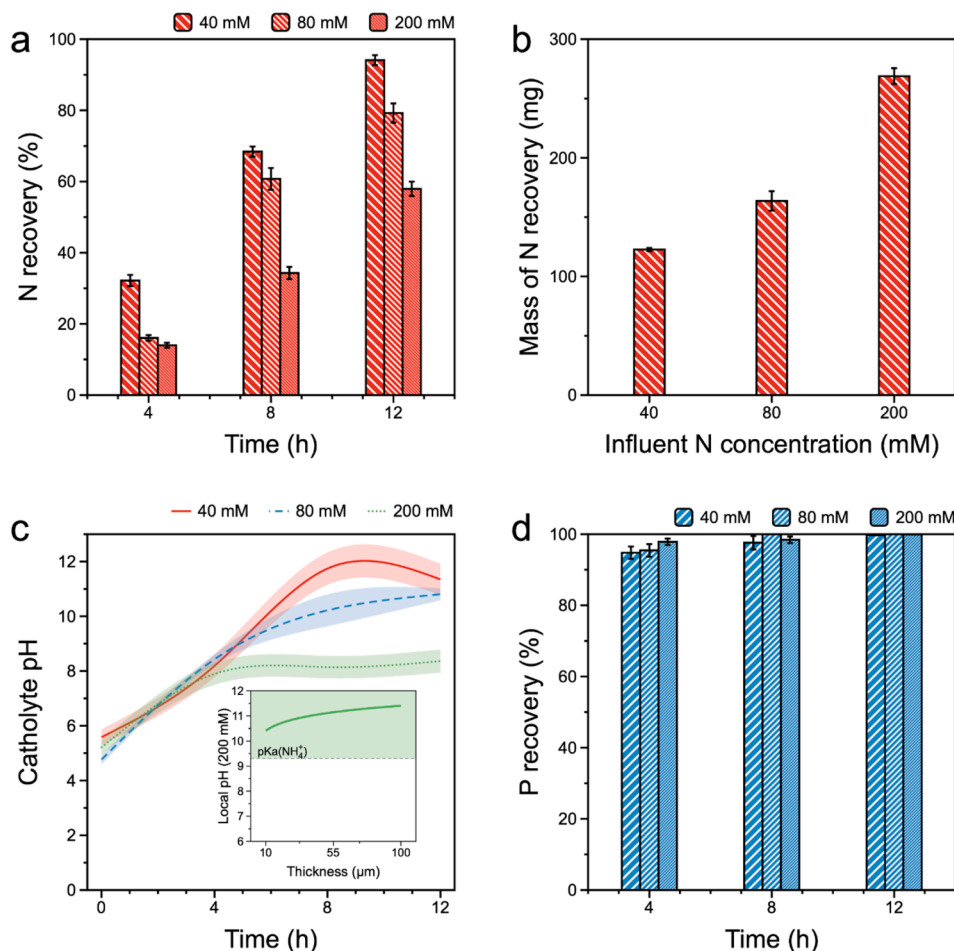


Fig. 4. Effects of influent N concentration on the concurrent recovery of N and P in the ECNRS: (a) N recovery efficiency; (b) N recovery mass; (c) catholyte pH and local pH near the cathode (200 mM N); and (d) P recovery efficiency. (40–200 mM N, 5 mM P, Ca/P = 2:1, and 4.0 V applied voltage).

possible to turn back to NH_4^+ especially the bulk pH was lower the pK_a (NH_4^+). This might cause the decrease of N recovery efficiency when we increased the influent P concentration.

3.3. Energy consumption and preliminary economic analyses of the concurrent N and P recoveries

The huge energy consumption and economics cost have always limited the practical application of N and P recoveries. Thus, we compared the energy consumption and economic analyses of the concurrent N and P recoveries process with former studies (Table 1) and the details are shown in Table S2-S4.

When we separately calculated the energy consumption for N recovery, the values were 14.6 ± 0.8 kWh/kg N for N recovery with a flux (across the GPM) of 47.3 ± 5.5 g $\text{NH}_3\text{-N}/(\text{m}^2\cdot\text{d})$. Carbon emission could be calculated as 9.43 kg $\text{CO}_2\text{-eq}/\text{kg N}$ by multiplying electricity consumption with emission factor of 0.65 kg $\text{CO}_2\text{-eq}/\text{kWh}$ [20]. In the catholyte, the concentration of N was about 10 times higher than that of P, which required continuous electric input for N recovery even though P was completely recovered within 8 h. Considering that N & P could be recovered simultaneously in the ECNRS, the energy input was used to generation acid and base for simultaneously supporting N and P recoveries. This is a process of killing several birds with one stone, which could offset a part of energy consumption and had an obvious advantage over the separate N or P recovery. The economic cost for the N and P recoveries should be assessed separately based on the chemical cost (mainly in the P recovery process) and the operational cost (mainly electric cost) (Eq. (4)). Electric input was almost used for pH elevation

and ammonium-ammonia transformation in this study. Thus, only chemical cost was taken into calculation for P recovery. The price of electricity was set as 0.10 \$/kWh. The cost of Ca source (based on the Ca/P molar ratio of 2:1) for P recovery was estimated in the form of $\text{Ca}(\text{OH})_2$ (0.13 \$/kg). Based on these, the cost of concurrent N and P recoveries in the ECNRS are 1.84 \$/kg N and 0.69 \$/kg P. Operational cost of the N recovery accounted for the main part of the total N recovery cost in the ES and ECNRS, which was greatly reduced compared with that of air stripping [25].

Moreover, the net energy consumption could be further reduced considering the generated hydrogen energy (4.3 kWh/kg N) [26]. Considering hydrogen energy offset, the carbon emission could be reduced to 6.32 kg $\text{CO}_2\text{-eq}/\text{kg N}$. In the P recovery via CaP crystallization, the recovery efficiency could be over 85 % even if the Ca/P molar ratio was less than 2:1 [27]. Therefore, the chemical cost of ECNRS for P recovery could be further reduced to less than 0.24 \$/kg P. Significantly, lower P concentration in the target wastewater for P recovery usually contributes to higher energy consumption and economic cost.

3.4. Implications

It can be seen from the above results that the ECNRS can achieve concurrent N & P recovery with enhanced N recovery and almost complete P recovery. Compared to other N or P recovery methods that require external acid and base inputs, the ECNRS doesn't require external inputs of acid and base, reducing the operation difficulty and economic cost. Energy consumption calculated separately for N recovery was still high but could be offset partially by the concurrent P recovery.

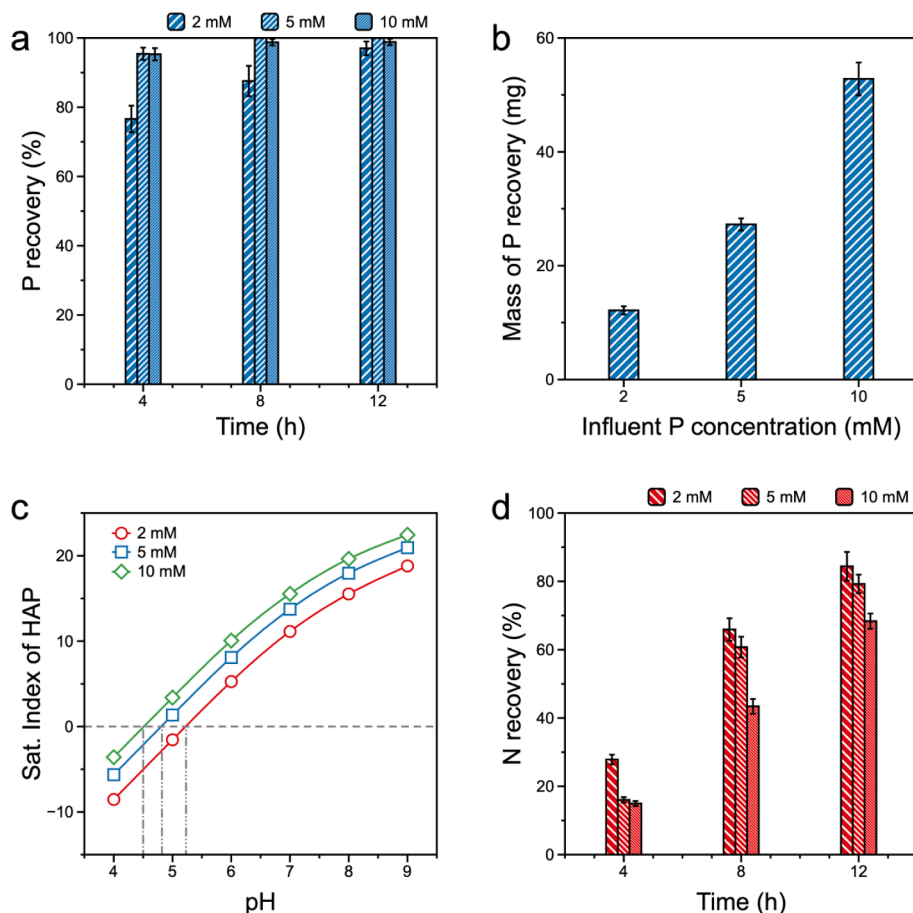


Fig. 5. Effects of influent P concentration on the concurrent recovery of N and P in the ECNRS: (a) P recovery efficiency; (b) P recovery mass; (c) saturation index of HAP in variable pH; and (d) N recovery efficiency. (80 mM N, 2–10 mM P, Ca/P = 2:1, and 4.0 V applied voltage).

Table 1

Comparison of energy consumption and economic cost among the processes for N and P recoveries.

	Recovery process	Influent	Concentration (mg N/L or mg P/L)	Energy consumption (kWh/kg)	Total cost (\$/kg)	Ref.
N recovery	Air stripping	Real urine	3800 (N)	19.8–25.6 (N)	2.73–3.19 (N)	[25]
	ES	AS ^a	3400 (N)	18.8 (N)	2.48 (N)	[28]
	BES	AS	1120 (N)	2.91 (N)	1.05 (N)	[19]
P recovery	CaP crystallization	SAD ^b	37 (P)	4.44 (P)	0.81–0.85 (P)	[27]
	Struvite crystallization	Real urine	310 (P)	70.76 (P)	7.78 (P)	[29]
	ES	DW ^c	7.7 (P)	110–2240 (P)	11–224 (P)	[30]
	BES	PS ^d	155 (P)	2.18 (P)	0.85 (P)	[18]
Concurrent N&P recovery	ECNRS	AS+PS	1120 (N), 155 (P)	14.6 (N), Negligible (P)	1.84 (N), 0.69 (P)	This study

^a AS: ammonium sulfate solution; ^b SAD: sludge anaerobic digestate; ^c DW: domestic wastewater; ^d PS: phosphate solution.

But benefit from the concurrent N and P recovery, the economic benefit of ECNRS operation could be over 300 % calculated according to Eq. (5) and Table S2. The concurrent recovery of N and P from the wastewater with high N/P ratios, such as source-separated urine, sludge digestate and animal manure digestate, is more suitable for the ECNRS. Taken source-separated urine as an example, its in-situ recovery by the ECNRS could reduce approximately 50 % of N in the influent of municipal wastewater treatment facility and furtherly 50 % external carbon source consumption for the denitrification process especially in China. Moreover, implementation of N recovery by ECNRS can also achieve carbon offset for N fertilizer manufacture industry. In the future work, it is planned to further examine the long-term performance of the system, membrane fouling (ion exchange membranes and GPM) and GPM wetting.

4. Conclusions

The present study realized the concurrent recovery of ammonia and phosphate by integrating TMCS and HAP crystallization in an electrochemical nutrients recovery system. The products can be used as the raw materials for N and P industries. The concurrent N and P recoveries process was found to obviously enhance the N recovery efficiency with almost complete P recovery. Increasing influent N or P concentration resulted in a prolonged time for the nutrients recovery, because the enhanced pH buffering delayed the pH rising of the catholyte. Thus, the concurrent N and P recoveries in the system showed cost-effective advantages beyond the previous methods for the process of wastewater with high N/P molar ratios.

Declaration of Competing Interest

The authors declare that they have no known competing financial interests or personal relationships that could have appeared to influence the work reported in this paper.

Acknowledgements

This work was sponsored by Natural Science Foundation of Shanghai (No. 20ZR1418900, No. 21ZR1468700), China; National Key R&D Program of China (No. 2021YFC3201301), China; and Fundamental Research Funds for the Central Universities, China.

Appendix A. Supplementary data

Supplementary data to this article can be found online at <https://doi.org/10.1016/j.cej.2022.140169>.

References

- [1] W.-F. Zhang, Z.-X. Dou, P. He, X.-T. Ju, D. Powlson, D. Chadwick, D. Norse, Y.-L. Lu, Y. Zhang, L. Wu, X.-P. Chen, K.G. Cassman, F.-S. Zhang, New technologies reduce greenhouse gas emissions from nitrogenous fertilizer in China, *PNAS*. 110 (21) (2013) 8375–8380.
- [2] D.P. Van Vuuren, A.F. Bouwman, A.H.W. Beusen, Phosphorus demand for the 1970–2100 period: A scenario analysis of resource depletion, *Glob. Environ. Change*. 20 (3) (2010) 428–439.
- [3] J. Al-Mallahi, R.Ö. Sürmeli, B. Çalli, Recovery of phosphorus from liquid digestate using waste magnesite dust, *J. Clean. Prod.* 272 (2020), 122616.
- [4] D. Cordell, J.-O. Drangert, S. White, The story of phosphorus: Global food security and food for thought, *Glob. Environmen. Change*. 19 (2009) 292–305.
- [5] J. Elser, E. Bennett, A broken biogeochemical cycle, *Nature*. 478 (7367) (2011) 29–31.
- [6] Z. Wang, J. Zhang, X. Guan, L. She, P. Xiang, S. Xia, Z. Zhang, Bioelectrochemical acidolysis of magnesite to induce struvite crystallization for recovering phosphorus from aqueous solution, *J. Environmen. Sci.* 85 (2019) 119–128.
- [7] H. Cruz, Y.Y. Law, J.S. Guest, K. Rabaey, D. Batstone, B. Laycock, W. Verstraete, I. Pikaar, Mainstream ammonium recovery to advance sustainable urban wastewater management, *Environ. Sci. Technol.* 53 (19) (2019) 11066–11079.
- [8] Z. Deng, N. van Linden, E. Guillen, H. Spanjers, J.B. van Lier, Recovery and applications of ammoniacal nitrogen from nitrogen-loaded residual streams: A review, *J. Environmen. Manage.* 295 (2021), 113096.
- [9] C.A. Cid, J.T. Jasper, M.R. Hoffmann, Phosphate recovery from human waste via the formation of hydroxyapatite during electrochemical wastewater treatment, *ACS Sustain. Chem. Eng.* 6 (3) (2018) 3135–3142.
- [10] J.L. Campos, D. Crutchik, Ó. Franchi, J.P. Pavissich, M. Belmonte, A. Pedrouso, A. Mosquera-Corral, Á. Val del Río, Nitrogen and phosphorus recovery from anaerobically pretreated agro-food wastes: A review, *Front. Sustain. Food Syst.* 2 (2019) 91.
- [11] F. Fasaei, J.H. Bitter, P.M. Slegers, A.J.B. van Bostel, Techno-economic evaluation of microalgae harvesting and dewatering systems, *Algal Res.* 31 (2018) 347–362.
- [12] T. Dockhorn, About the economy of phosphorus recovery, in: *International Conference on Nutrient Recovery From Wastewater Streams*, IWA Publishing, London, UK, 2009, pp. 145–158.
- [13] R.D. Cusick, M.L. Ullery, B.A. Dempsey, B.E. Logan, Electrochemical struvite precipitation from digestate with a fluidized bed cathode microbial electrolysis cell, *Water Res.* 54 (2014) 297–306.
- [14] H. Huang, P. Zhang, Z. Zhang, J. Liu, J. Xiao, F. Gao, Simultaneous removal of ammonia nitrogen and recovery of phosphate from swine wastewater by struvite electrochemical precipitation and recycling technology, *J. Clean. Prod.* 127 (2016) 302–310.
- [15] P. Kuntke, M. Rodrigues, T. Sleutels, M. Saakes, H.V.M. Hamelers, C.J.N. Buisman, Energy-efficient ammonia recovery in an up-scaled hydrogen gas recycling electrochemical system, *ACS Sustain. Chem. Eng.* 6 (6) (2018) 7638–7644.
- [16] Y. Lei, M. Saakes, R.D. van der Weijden, C.J.N. Buisman, Electrochemically mediated calcium phosphate precipitation from phosphonates: Implications on phosphorus recovery from non-orthophosphate, *Water Res.* 169 (2020), 115206.
- [17] M.K. Perera, J.D. Englehardt, Simultaneous nitrogen and phosphorus recovery from municipal wastewater by electrochemical pH modulation, *Sep. Purif. Technol.* 250 (2020), 117166.
- [18] Z. Wang, J. Zhang, X. Hu, R. Bian, Y. Xv, R. Deng, Z. Zhang, P. Xiang, S. Xia, Phosphorus recovery from aqueous solution via a microbial electrolysis phosphorus-recovery cell, *Chemosphere*. 257 (2020), 127283.
- [19] Z. Zhang, Z. Wang, J. Zhang, R. Deng, H. Peng, Y. Guo, P. Xiang, S. Xia, Ammonia recovery from wastewater using a bioelectrochemical membrane-absorbed ammonia system with autigenic acid and base, *J. Clean. Prod.* 296 (2021), 126554.
- [20] H. Wang, Y. Yang, A.A. Keller, X. Li, S. Feng, Y. Dong, F. Li, Comparative analysis of energy intensity and carbon emissions in wastewater treatment in USA, germany, china and south africa, *Appl. Energy*. 184 (2016) 873–881.
- [21] Y. Lei, M. Saakes, R.D. van der Weijden, C.J.N. Buisman, Effects of current density, bicarbonate and humic acid on electrochemical induced calcium phosphate precipitation, *Chem. Eng. J.* 342 (2018) 350–356.
- [22] T.H. Muster, J. Jermakka, Electrochemically-assisted ammonia recovery from wastewater using a floating electrode, *Water Sci. Technol.* 75 (2017) 1804–1811.
- [23] C. Zhang, J. Ma, T.D. Waite, The impact of absorbents on ammonia recovery in a capacitive membrane stripping system, *Chem. Eng. J.* 382 (2020), 122851.
- [24] D. Hou, A. Iddya, X.i. Chen, M. Wang, W. Zhang, Y. Ding, D. Jassby, Z.J. Ren, Nickel-based membrane electrodes enable high-rate electrochemical ammonia recovery, *Environ. Sci. Technol.* 52 (15) (2018) 8930–8938.
- [25] B. Liu, A. Giannis, J. Zhang, V.-C. Chang, J.-Y. Wang, Air stripping process for ammonia recovery from source-separated urine: Modeling and optimization, *J. Chem. Technol. Biotechnol.* 90 (12) (2015) 2208–2217.
- [26] A.K. Luther, J. Desloover, D.E. Fennell, K. Rabaey, Electrochemically driven extraction and recovery of ammonia from human urine, *Water Res.* 87 (2015) 367–377.
- [27] S. Daneshgar, A. Buttafava, A. Callegari, A.G. Capodaglio, Economic and energetic assessment of different phosphorus recovery options from aerobic sludge, *J. Clean. Prod.* 223 (2019) 729–738.
- [28] W.A. Tarpeh, J.M. Barazesh, T.Y. Cath, K.L. Nelson, Electrochemical stripping to recover nitrogen from source-separated urine, *Environ. Sci. Technol.* 52 (3) (2018) 1453–1460.
- [29] S. Antonini, S. Paris, T. Eichert, J. Clemens, Nitrogen and phosphorus recovery from human urine by struvite precipitation and air stripping in vietnam, *CLEAN – Soil, Air, Water*. 39 (2011) 1099–1104.
- [30] Y. Lei, J.C. Remmers, M. Saakes, R.D. van der Weijden, C.J.N. Buisman, Influence of cell configuration and long-term operation on electrochemical phosphorus recovery from domestic wastewater, *ACS Sustain. Chem. Eng.* 7 (7) (2019) 7362–7368.